NUMERICAL INVESTIGATION OF THE CAVITATION IN PUMP INDUCER

Mishaal A. AL-Saffar
Mechanical Department
College of Engineering
AL-Mustansiriya University.

Najdat N. Abdulla
Mechanical Department
College of Engineering
University of Baghdad.

Jalal M. Jalil
ElectroMechanical
Engineering Department
University of Technology.

ABSTRACT

A numerical investigation of the non-cavitating and cavitating performance of a three-blade pump inducer under nominal and off-design operating conditions is presented. Three different simulated hydrofoils; a flat plate, "NACA0004", and "Clark-Y-6%" has been selected to represent the profile of the inducer blade. A 2D, steady, incompressible, turbulent, and isothermal flow field between the inducer blades is simulated using the FVM. The "Interface Tracking" model is selected to predict the cavity profile of the attached cavitation and the cavitating performance drop. For each blade profile, the influence of solidity in the range of (1.8 to 3.0) and blade angle in the range of $(20^{°}$ to $35^{°})$ on the inducer performance is studied. Comparing the present model with available experimental and numerical results, confirms that the developed model well predicts the general non-cavitating performance for an inducer having a flat plate blade profile. For "NACA0004", or "Clark-Y-6%" hydrofoil blade profiles, a reduction in the operating range of these inducers is produced. In addition, the developed model predicts the inception of cavitation earlier than the experimental results. The predicted cavitating head drop curve of an inducer having a flat plate blade profile is compared with available experimental results and a good agreement is obtained. The drop curve occurs suddenly and simultaneously with the experimental one. For "NACA0004", or "Clark-Y-6%" hydrofoil blade profiles, a smooth curves with simultaneous or gradual head drop occurs with the experimental one, respectively. Generally, the agreement between the results is satisfactory.

الخلاصة

تم عرض دراسة عددية عن خصائص الأداء لمحاثة ثلاثية الريش لمضخة تعمل عند انعدام التكهف ومع التكهف عند حالات العمل التصميمية وغير التصميمية. تم اختيار ثلاثة أشكال بطريقة منمذجة لمطيار مائي وهي: صفيحة مستوية، و "NACA0004" و "Clark-Y-6%" لتمثل شكل ريشة المحاثة. تمت نمذجة الجريان ثنائي الأبعاد, مستقر, غير انضغاطي, مضطرب، و ذو درجة حرارة ثابتة لمائع ينساب بين ريش المحاثة وباستخدام طريقة الحجم المحددة. تم اختيار نموذج "Interface Tracking" لتخمين شكل الفجوة للتكهف الملتصق و انخفاض الأداء المتكهف. لكل شكل ريشة، تمت دراسة تأثير الصلادة في المدى (1.8 الى 3.0) وزاوية الريشة في المدى (20 الى 35 درجة) على أداء المحاثة. إن مقارنة النتائج التي تم الحصول عليها من النموذج المطور مع النتائج المتوفرة من التجارب العملية ومن الحسابات العددية ,تؤكد أن النموذج المطور يحسن تخمين الأداء العام وبدون تكهف لمحاثة ذات ريشة بشكل صفيحة مستوية. لمطيار مائي بشكل "NACA0004" أو "Clark-Y-6%" سينخفض مدى التشغيل لهذه المحاثات. بالإضافة إلى ذلك, فان النموذج المطور يخمن بدء التكهف بصورة مبكرة عن تلك المتوفرة من التجارب العملية. تمت مقارنة منحني انخفاض الضغط عند تكهف المحاثة ذات ريشة بشكل صفيحة مستوية مع النتائج المتوفرة من التجارب العملية حيث تم الحصول

على توافق جيد. إن منحني انخفاض الضغط يحدث بشكل مفاجئ ومتزامن مع نضيره المتوفر من التجارب العملية. لمطيار مائي بشكل "NACA0004" أو "Clark-Y-6%" , فان منحنيا انخفاض الضغط تحدث بشكل متزامن أو تدريجي مع نضيرها المتوفر من التجارب العملية وعلى التوالي. بشكل عام, إن التوافق بين النتائج هو مرضي.

KEYWORDS

Cavitation, inducer, two-phase, Rayleigh-Plesset, NACA0004, Clark-Y-6%, interface tracking, FVM.

INTRODUCTION

Nowadays, satellite systems such as satellite broadcasting and navigation by GPS are becoming indispensable for our life. Liquid fuel rockets are mainly used to launch the satellites. In the rockets, liquefied hydrogen (LH_2) and liquefied oxygen (LOX) are used as propellants. A turbopump, which supplies the propellants to a combustion chamber with high pressure, is incorporated in the rocket engine to make the system smaller and lighter, **(Tokumasu et. al. 2003)**. It is necessary for the turbopump to run very fast to make it smaller. In this condition, cavitation occurs, because the local static pressure becomes smaller than the vapor pressure.

The performance of the pump, or other hydraulic device, may be significantly degraded. In the case of pumps, there is generally a level of inlet pressure at which the performance will decline dramatically, a phenomenon termed "Cavitation breakdown". This adverse effect has naturally given rise to changes in the design of a pump to minimize the degradation of the performance; or, to put it another way, to optimize the performance in the presence of cavitation. One such design modification is the addition of a cavitating inducer upstream of the inlet to a centrifugal or mixed flow pump impeller. Another example is manifest in the blade profiles used for super-cavitating propellers. These super-cavitating hydrofoil sections have a sharp leading edge, and are shaped like curved wedges with a thick, blunt trailing edge.

An inducer is attached to these turbopumps to increase their efficiency. The "inducer" is a device that causes a rise in the inlet head, which prevents cavitation in a pump stage following the inducer. Inducers are therefore used at the inlet portion of the main pump. They are typically designed to be axial flow impellers with a high solidity so that long narrow passages result. Cavitation bubbles collapse in these passages before they reach the main pump, **(Acosta 1958)**.

Nowadays, CFD numerical techniques are commonly used in the hydraulic design of industrial turbomachines components. Unfortunately, without a suitable numerical model, it is impossible to solve directly cavitating flows. Since 1990's, various methods have been proposed to simulate cavitating flows as two-phase flows. Three different approaches have been mainly proposed for the numerical simulation of cavitation phenomenon in hydraulic machinery, these are: (1) The Single Fluid Model: It is based on a pseudo-density function of the liquid-vapor mixture to close the equations system. A Baratropic law relating the pressure to density is mainly proposed. Assuming no-slip is present between the liquid and vapor phases, both phases are in thermal equilibrium. **(Coutier-Delgosha et. al. 2001)** has used this model to simulate numerically the cavitation behavior of beveled and sharp leading edge shapes for two-dimensional hydrofoil sections of an inducer blade at two different angles of attacks. This simulation was coded with the 3D "FINE/TURBO™" commercial code. **(Joussellin et. al. 2001)** has used this model to investigate numerically the cavitating flows in rocket engine turbopump inducers. A 2D numerical model of unsteady cavitation, developed by previous studies, was applied to a 2D blade cascade drawn from the inducer geometry. **(Coutier-Delgosha et. al. 2002)** has used this model to investigate numerically the characteristics, performance breakdown, cavitation development and vapor structures distribution of a 4-blade turbopump inducer in non-cavitating and cavitating conditions associated with quasi-steady effects. The numerical model was

coded using the "FINE/TURBO™" commercial code. (2) The "VOF" Model: It is a multiphase mixture model which has an additional equation for the volume fraction including source terms to model the vaporization and condensation processes. Using a truncated form of the Rayleigh-Plesset equation to estimate the rate of vapor production or destruction assuming that thermal and mechanical equilibrium stands between liquid and vapor phases. **(Bakir et. al. 2003)** has used this model to investigate numerically the hub shape effect on the inducers performance under cavitation. **(Reboud et. al. 2003)** has used this model to correctly simulate the unsteady cavitaing flows in 2D venturi type section implementing the influence of four turbulence models. Simulations were also performed to a hydrofoil, a foil cascade, and another venturi type section. **(Ait-Bouziad et. al. 2004)** has used this model to simulate the cavitation behavior of a 3-blade industrial inducer. **(Bakir et. al. 2004)** developed a numerical cavitation model suitable for general three-dimensional flows with extensive cavitation at large density ratios. His model assumed two-phase, three-component system with no inter-phase slip and thermal equilibrium between any of the components and phases. (3) The "Interface Tracking" Model: In this approach, the cavity interface is considered as a free surface boundary of the computation domain and the computational grid includes only the liquid phase. **(Hirschi et. al. 1998)** has used this model to predict the performance drop of a cavitating centrifugal pump and the influence of the diffuser geometry on this performance. **(Ait-Bouziad et. al. 2003)** investigated numerically the performance of "Interface Tracking" and "VOF" Models for modeling the cavitation phenomenon in the case of 3-blade industrial inducer.

This paper is presented to study and simulate numerically the non-cavitating and cavitating performance of a three-blade pump inducer under nominal and off-design operating conditions and to predict the cavity profile using the FVM. This inducer will be designed for nominal operating condition with flow coefficient (φ=0.38), rotational speed (N=1450 rpm), and head coefficient (ψ=0.15). The "Interface Tracking" model is selected to predict the cavity profile of the attached cavitation and the cavitating performance drop. Three different simulated hydrofoils; a flat plate, "NACA0004" and "Clark-Y-6%" will be selected to represent the shape of the three-blade inducer. For each blade profile, the influence of solidity in the range of (1.8 to 3.0) and blade angle in the range of (20° to 35°) on the inducer non-cavitating and cavitating performance will be studied under nominal and off-design operating conditions. The results of this paper will be compared with available experimental and numerical results of the "CFX-TASCflow" commercial code.

The details of this paper are described completely in a Ph.D. Thesis work of **(AL-Saffar 2007)**.

GOVERNING EQUATIONS

The two-dimensional governing equation of mass and momentum for steady, turbulent, incompressible flow can be written in tensor conservative form and expressed in Cartesian coordinates as follows, **(Nilsson 2002)**:

$$\frac{\partial u_i}{\partial x_i} = 0 \tag{1}$$

$$\rho_L \frac{\partial u_i u_j}{\partial x_j} = -\frac{\partial p}{\partial x_i} + \frac{\partial \left(t_{ij} + \tau_{ij} \right)}{\partial x_j} \tag{2}$$

Where (t_{ij}), is the viscous shear stress tensor that is expressed as:

$$t_{ij} = \mu \left[\left(\frac{\partial u_i}{\partial x_j} + \frac{\partial u_j}{\partial x_i} \right) - \frac{2}{3} \left(\frac{\partial u_k}{\partial x_k} \delta_{ij} \right) \right] \tag{3}$$

The Reynolds stress tensor (τ_{ij}) can be determined according to the Boussineq assumption as:

$$\tau_{ij} = -\overline{\rho_L u_i' u_j'} = \mu_t \left[\left(\frac{\partial u_i}{\partial x_j} + \frac{\partial u_j}{\partial x_i} \right) - \frac{2}{3} \left(\frac{\partial u_k}{\partial x_k} \delta_{ij} \right) \right] - \frac{2}{3} \delta_{ij} \rho_L k \tag{4}$$

The standard (k-ε) two-equation turbulence model has been selected among other turbulence models. Hence, the value of the turbulent eddy viscosity (μ_t) is estimated as, **(Wang and Komori 1998)**:

$$\mu_t = \frac{c_\mu \rho_L k^2}{\varepsilon} \tag{5}$$

"INTERFACE TRACKING" MODEL:

It is a mono-fluid model having an incompressible, single-phase transport equation, and it considers the cavity interface as a free surface boundary of the computational domain. As the cavity shape has an influence on the mean flow, an iterative process needs to be applied between the CFD code and the cavitation prediction one to modify the interface shape in order to reach a constant pressure equal to the vapor pressure along it. This shape is defined by the envelope of high number of transferred bubbles over the blade associated with attached cavitation; the bubble radius instead of its diameter is used to define this envelope. The main numerical complexity is how to predict an adaptive grid for the computational domain to update the cavity shape. This model does not compute any cavitation, which is not attached to the blade surface. Only the attached cavitation to the blade surface boundary is predicted, and the tip clearance cavitation is not considered.

This model has the advantage of being independent of the flow computation code. It is based on some version of the Rayleigh-Plesset equation that defines the relation between the radius of a spherical bubble, (R), and the pressure, (p), far from the bubble. The generalized Rayleigh-Plesset equation for bubble dynamics is given as, **(Brennen 1995, 2005)**:

$$\frac{p_v - p}{\rho_L} = R \frac{d^2R}{dt^2} + \frac{3}{2} \left(\frac{dR}{dt} \right)^2 + \frac{4v_L}{R} \frac{dR}{dt} + \frac{2S}{\rho_L R} \tag{6}$$

In the absence of the surface tension and viscous terms, the generalized form of this equation is truncated to predict (R) at a given (p), provided that (p_v) is known.

$$\frac{dR}{dt} = \sqrt{\frac{2}{3} \frac{(P_v - P)}{\rho_L}} \tag{7}$$

NUMERICAL TECHNIQUE

The "Interface Tracking" model has been used to simulate the hydraulic performance of a cavitating performance of a three-blade pump inducer under nominal and off-design operating

conditions using the FVM using the standard k-ε turbulence model associated with laws of the wall along solid boundaries. Steady state solutions were obtained by setting a uniform flow velocity and a constant total pressure at the inducer inlet for the boundary conditions.

A grid independency test for the three selected profiles is performed and a single-block structured mesh has been generated for each profile. Mesh sizes of (30x100), (30x99) and (30x70) are selected for flat plate, "NACA0004" hydrofoil profile and "Clark-Y-6%" hydrofoil respectively. Each mesh is made for a single passage (1/3 of the inducer).

Computations starts from the non-cavitating regime, then the "Interface Tracking" model is turned on, while the imposed total pressure at the channel inlet is decreased by a constant step of (10,000 Pa). Close to the drop zone, this step is reduced by a factor of (10) and more to overcome the high instability of the solution due to the strong non-linear behavior of the cavitation phenomenon. For each value of the imposed total pressure at the channel inlet and after entering the drop zone, the truncated Rayleigh-Plesset equation is activated to predict the cavity interface shape. The cavity interface is treated as a wall boundary of the blade-to-blade channel. Hence, the wall function will be imposed along the cavity interface. This is considered to be a major assumption of the "Interface Tracking" model. The shape of the cavity interface is inserted into the grid generator to update the grid shape. This shape is adapted step by step according to the pressure distribution obtained from the flow computation at the previous iteration in order to reach a given condition (the pressure at the cavity interface is equal to the vapor pressure). The head drop curve is created gradually. It is noted finally that the time consuming for the creation of a whole one head drop curve is about (30 min) on a P4, Celeron(R) CPU, 2.41 GHz, 256 MB of RAM. For all computations, a maximum residual is kept below 10^{-4}.

RESULTS DISCUSSION

Non-Cavitating Performance

The effects of different values of solidity and blade angle on the numerical results of the (Head-Flow) curve for the non-cavitating performance of an inducer having a flat plat, "NACA0004", and "Clark-Y-6%" hydrofoil blade profile are simulated and compared with the experimental and 3D numerical results of, **(Bakir et. al. 2004)**, using the "CFX-TASCflow" commercial code, of the "LEMFI" inducer, as shown in **Fig. 1**. For each case study, the optimum simulated values of solidity and blade angle are listed in **Table 1**.

Table (1) Optimum geometry configuration for different simulated shapes of blade profiles.

Case study	Blade profile	Optimum geometry configuration	
		Solidity (s)	**Blade angle (β_b)**
1	Flat plate	2.95	25°
2	"NACA0004"	2.95	30°
3	"Clark-Y-6%"	1.8	25°

As shown in **Fig. 1**, for the flat plate case study, a good agreement between the experimental results of **(Bakir et. al. 2004)** of "LEMFI" inducer, and the numerical results of the present work is obtained at nominal flow coefficient (φ=0.38), and high flow coefficents. At low flow coefficients, an average difference in the value of head coefficient of about (0.15) is obtained between the experimental

and two-dimensional numerical results and this due to the tip clearance effects. For "NACA0004" or "Clark-Y-6%" hydrofoil blade profiles using the optimum values of solidity and blade angle listed in **Table 1**, will result a reduction in the operating range producing a flow coefficient value of (10%) lower than that of the nominal one with an average head coefficient value of (30%) higher than that of the nominal one. This is due to the change in the blade profile and geometric parameters.

Cavitation Inception

Fig. 2 shows the comparison between the experimental and numerical results of **(Bakir et. al. 2004)** of "LEMFI" inducer, for the inception cavitation number (σ_i) versus flow coefficient (φ) and present work inducer having different simulated shapes of hydrofoil profiles, using the optimum solidity and blade angle values listed in **Table 1**. As shown, the present work numerical results predict the inception of cavitation earlier than the experimental and numerical results of **(Bakir et. al. 2004)**. This is due to the unsteady nature of cavitation inception. On the other hand, the numerical results of **(Bakir et. al. 2004)** were based on using the "VOF" model and the inception cavitation number was associated with a (3%) head drop.
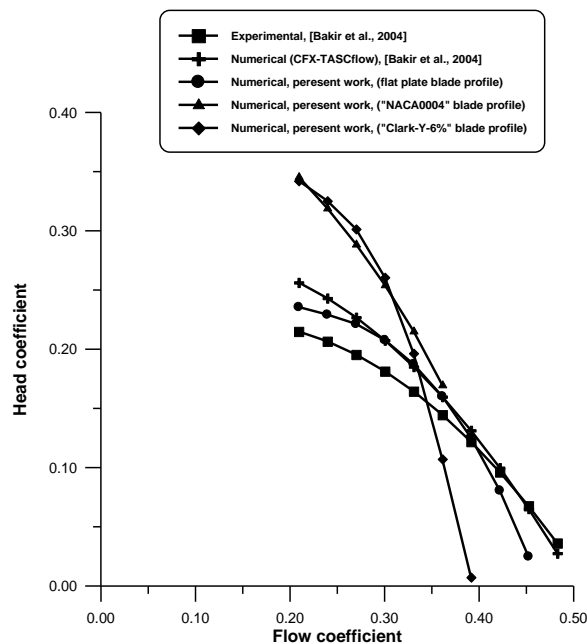
Fig. 1 : Non-cavitating performance.
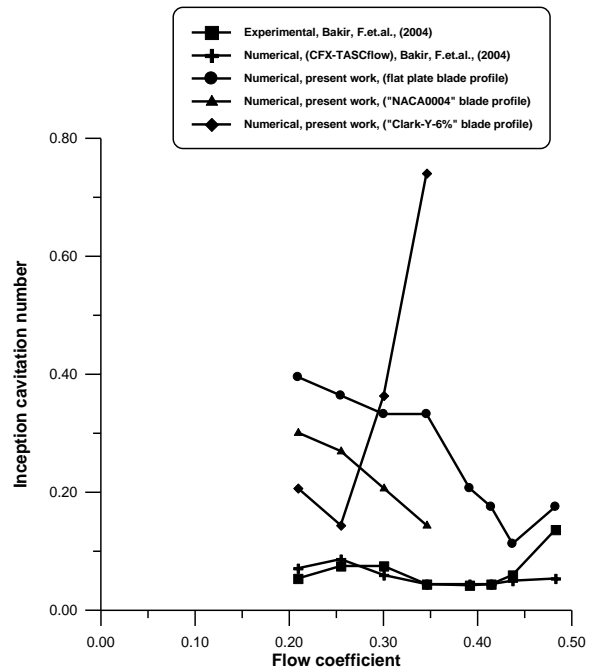
Fig. 2 : Cavitation inception curve.

Cavitating Performance

Fig. 3 and **Fig. 4** show the comparison between the developed model and the experimental and numerical results of **(Bakir et. al. 2004)**, for the head drop characteristics of an inducer having a flat plate blade shape, operating at a flow coefficient of (φ=0.346) or (φ=0.38), a good agreement is obtained between the developed model and experimental results. The drop curve occurs suddenly and simultaneously with the experimental one. The agreement between the results is very satisfactory.

For "NACA0004" hydrofoil profile, when operating at a flow coefficient of (φ=0.346), a smooth with simultaneous head drop occurs with the experimental one, with a (30%) increase in the value of the head coefficient.

For "Clark-Y-6%" hydrofoil, a smooth with gradual head drop occurs before the experimental one, with a (30%) increase in the value of the head coefficient, as shown in **Fig. 4**.
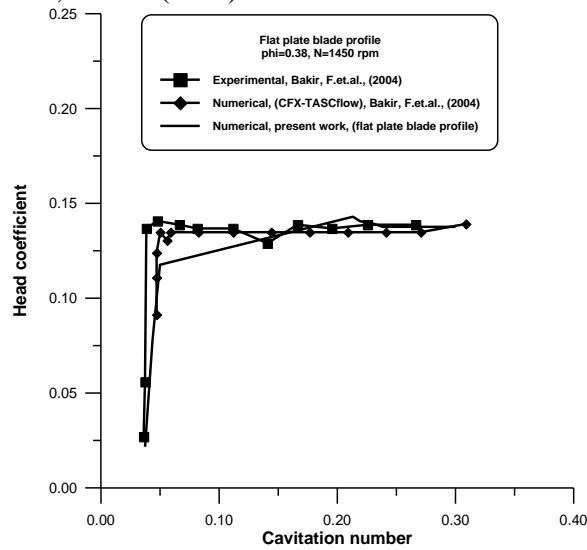
Fig. 3 : Head drop curve, φ=0.38
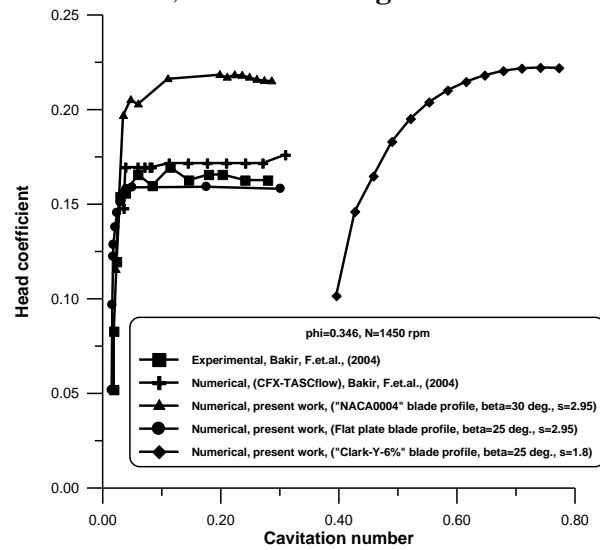
Fig. 4 : Head drop curve, φ=0.346

Fig. 5 show the evolution of the cavity profile on the suction side of a flat plate blade profile of an inducer operating at a flow coefficient of (φ=0.38) and (φ=0.346), at cavitation inception and with different cavitation numbers.
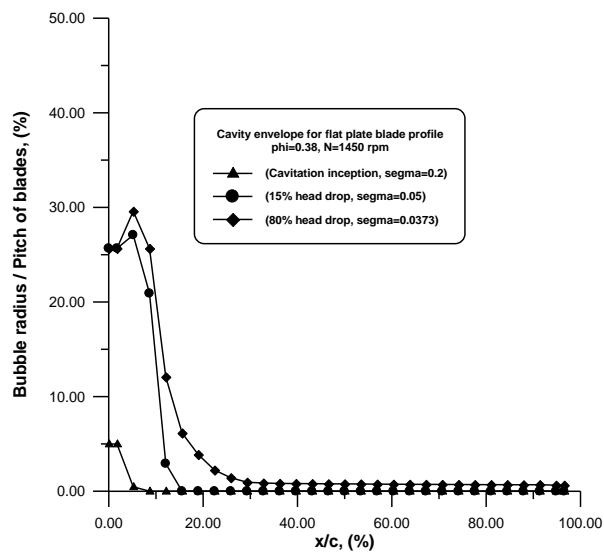
(a) Flat plate blade profile, φ=0.38
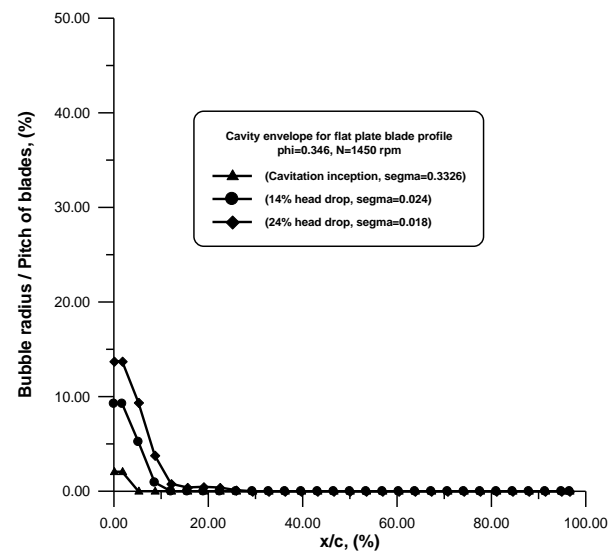
(b) Flat plate blade profile, φ=0.346

Fig. 5 : Cavity envelope evolution on the suction side at different cavitation numbers.

(a) "NACA0004" blade profile, φ=0.346   (b) "Clark-Y-6%" blade profile, φ=0.346
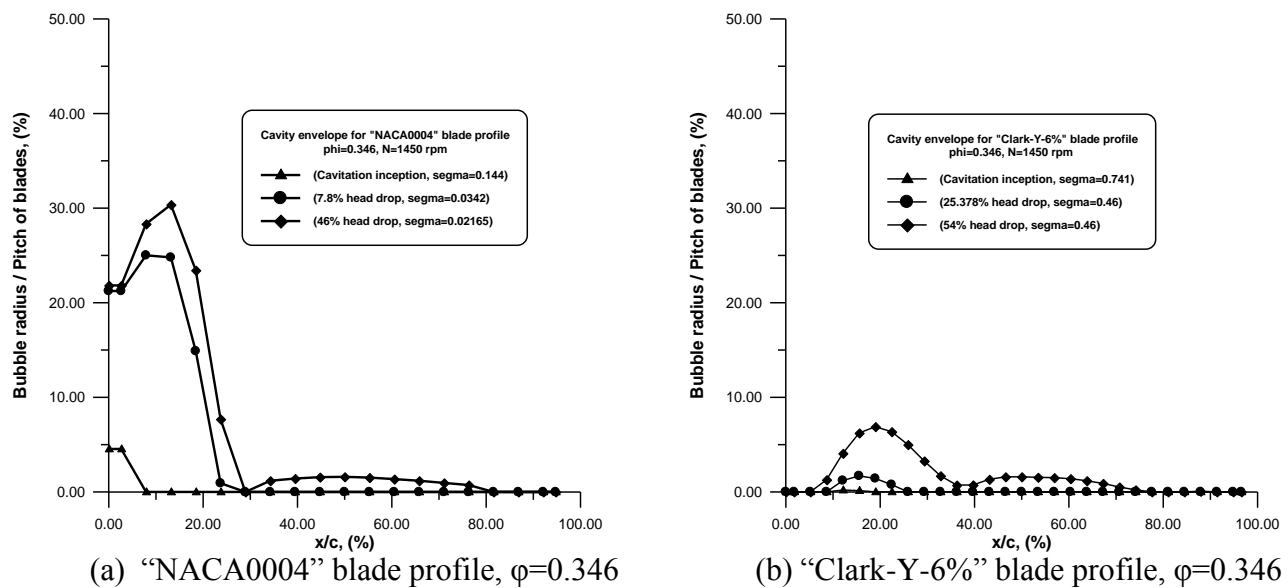
Fig. 6 : Cavity envelope evolution on the suction side at different cavitation numbers.

Fig. 6 shows the evolution of the cavity profile on the suction side of a "NACA0004" and "Clark-Y-6%" blade profile of an inducer operating at a flow coefficient of (φ=0.346), at cavitation inception and with different cavitation numbers.

CONCLUSIONS

The abnormal cavitating behavior of the "Clark-Y-6%" hydrofoil blade profile as shown in **Fig. 2** and **Fig. 4** is due to that the "Clark-Y-6%" hydrofoil blade profile is of cambered shape with a maximum thickness to cord ratio value of (6%) which is greater than that of the flat plate blade profile of a negligible constant thickness to cord ratio value and greater than the "NACA0004" hydrofoil blade profile of a symmetric shape with a maximum thickness to cord ratio value of (4%). This shape of the "Clark-Y-6%" hydrofoil blade profile will produce a greater contraction (i.e. a 2% increase above that of the "NACA0004" hydrofoil and a 6% increase above that of the flat plate shape) at its blade-to-blade channel resulting a higher velocity value at its throat and a lower pressure value which result a higher value of the inception of cavitation parameter and also a smooth with gradual head drop occurs before the head drop curve of both the "NACA0004" and the flat plate hydrofoils when operating at a flow coefficient of a value of (φ=0.346).

In general, the shape of the blade profile and its geometric parameters (i.e. the solidity and the blade angle values) has a major effect on the performance characteristics of the non-cavitating and cavitating pump inducer. Therefore, it is better to design and manufacture an inducer with a blade profile that produce a blade-to-blade channel that has no contraction (i.e. flat plate blade profile) having a relatively high value of solidity and a value of blade angle that produce a few degrees of the angle of incidence.

SYMBOLS AND ABBREVIATIONS

c=Cord length, (m).
c_μ= Empirical coefficient, (-).
h=Pitch of blades, (m).
k= Turbulent kinetic energy, (J/kg).
p= Static pressure, (Pa).
p_{in}=Inlet pressure, (Pa).
p^T= Total pressure, (Pa).
p_v= Vapor pressure, (Pa).
Q= Volumetric flow rate, (m^3/s).
R= Bubble radius, (m).
R_{hub}=Hub radius, (m).
R_{tip}= Tip radius, (m).
s= Solidity=c/h, (-).
S= Surface tension, (N/m).
t= Time, (s).
u= Cartesian velocity component, (m/s).
x= Cartesian coordinate, (m).

β_b= Blade angle, (degree).
$\delta_{ij=}$ Kroneker delta switch.
ε= Turbulent kinetic energy dissipation rate term, (J/kg).
μ= Dynamic viscosity, (N.s/m$^{2)}$).
$\mu_{t=}$ Turbulent eddy viscosity, (N.s/m^2).
ν_L= Kinematic viscosity, (m^2/s).
ρ_L=Liquid Density, (kg/m$^{3)}$).
σ= Cavitation parameter=$(p_{in}-p_v)/(0.5\rho_L\Omega^2 R^2_{tip})$, (-).
τ_{ij}= Reynolds stress tensor, (N/m$^{2)}$).
φ= Flow coefficient=$Q/(\pi\Omega R^3_{tip}[1-(R_{hub}/R_{tip})^2])$, (-).
ψ= Head coefficient= $(P_2^T-P_1^T)/(\rho_L\Omega^2 R^2_{tip})$, (-).
Ω= Angular velocity, (rad/s).
CFD= Computational Fluid Dynamics.
FVM= Finite Volume Method.
GPS= Global Positioning System.
LEMFI=Laboratoire d'Energétique et de Mécanique des Fluides Interne.
LOX= Liquefied Oxygen.
VOF= Volume Of Fluid.

REFERENCES

-Acosta, A.J., 1958, "An experimental study of cavitation inducers", Proceedings of 2nd Symposium on Navel Hydrodynamics, Washington D.C., pp. 533-557.

-Ait-Bouziad, Y., Farhat, M., Guennoun, F., Kueny, J.L., Avellan, F., 2003, "Physical modeling and simulation of leading edge cavitation, application to an industrial inducer", Fifth International Symposium on Cavitation (CAV2003), (cav03-os-6-014), Osaka, Japan, November 1-4.

-Ait-Bouziad, Y., Farhat, M., Kueny, J.L., Avellan, F., Miyagawa, K., 2004, "Experimental and numerical cavitation flow analysis of an industrial inducer", 22nd IAHR Symposium on Hydraulic Machinery and Systems, June 29 - July 2, Stockholm – Sweden.

-AL-Saffar, M.A., 2007, "Numerical investigation of the cavitation in pump inducer", Ph. D. Thesis, Mechanical Department, College of Engineering, University of Baghdad, Iraq.

-Bakir, F., Kouidri, S., Mejri, I., Rey, R., 2003, "Hub shape effects under cavitation on the inducers performance", Fifth International Symposium on Cavitation (cav2003), (Cav03-OS-6-001), Osaka, Japan, November 1-4.

-Bakir, F., Rey, R., Gerber, A.G., Belamri, T., Hutchinson, B., 2004, "Numerical and experimental investigations of the cavitating behavior of an inducer", International Journal of Rotating Machinery, 10: 15-25.

-Brennen, C.E., 1995, "Cavitation and bubble dynamics", Oxford University Press.

-Brennen, C.E., 2005, "Fundamentals of multiphase flows", Cambridge University Press.

-Coutier-Delgosha, O., Morel, P., Fortes-Patella, R., Reboud, J.L., 2002, "Numerical simulation of turbopump inducer cavitating behavior", IJRM paper No. 02-Y-56, (Previously presented at ISROMAC-9 Conference, Honolulu).

-Coutier-Delgosha, O., Reboud, J.L., Fortes-Patella, R., 2001, "Numerical study of the effect of the leading edge shape on cavitation around inducer blade sections", Forth International Symposium on Cavitation (CAV2001, session B7.003), California Institute of Technology, Pasadena, California, USA, 20-23 June.

-Hirschi, R., Dupont, Ph., Avellan, F., Favre, J.-N., Guelich, J.-F., Parkinson, E., 1998, "Centrifugal pump performance drop due to leading edge cavitation : Numerical predictions compared with model tests", Journal of Fluid Engineering, Vol. 120, pp 705-711, December.

-Joussellin, F., Courtot, Y., Coutier-Delgosha, O., Reboud, J.L., 2001, "Cavitating inducer instabilities: Experimental analysis and 2D numerical simulation of unsteady flow in blade cascade", Forth International Symposium on Cavitation (CAV2001, session B8.002), California Institute of Technology, Pasadena, California, USA, 20-23 June.

-Nilsson, H., 2002, "Numerical investigation of turbulent flow in water turbines", Ph.D. Thesis, Chalmers University of Technology, Sweden.

-Reboud, J.L., Coutier-Delgosha, O., Pouffary, B., Fortes-Patella, R., 2003, "Numerical simulation of unsteady cavitating flows: Some applications and open problems", Fifth International Symposium on Cavitation (CAV2003), (CAV2003-IL-10), Osaka, Japan, November 1-4.

-Tokumasu, T., Sekino, Y., Kamijo, K., 2003, "A new modeling of sheet cavitation considering the thermodynamic effects", Fifth International Symposium on Caviation, (Cav03-GS-16-003), Osaka, Japan, November 1-4.

-Wang, Y., Komori, S., 1998, "Prediction of duct flows with a pressure-based Procedure", Journal of Numerical Heat Transfer, Part A, Applications, Vol. 33, No. 7, pp.723-748, Taylor & Francis, London.